

Expedient Total Synthesis of Small to Medium-Sized Membrane Proteins via Fmoc Chemistry

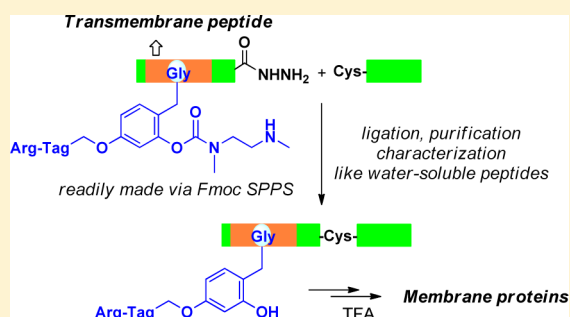
Ji-Shen Zheng,^{†,‡} Mu Yu,[‡] Yun-Kun Qi,[†] Shan Tang,[†] Fei Shen,[†] Zhi-Peng Wang,[†] Liang Xiao,[‡] Longhua Zhang,[‡] Chang-Lin Tian,^{*,‡} and Lei Liu^{*,†}

[†]Tsinghua-Peking Center for Life Sciences, Key Laboratory of Bioorganic Phosphorus Chemistry & Chemical Biology (Ministry of Education), Department of Chemistry, Tsinghua University, Beijing 100084, China

[‡]High Magnetic Field Laboratory, Chinese Academy of Sciences and School of Life Sciences, University of Science and Technology of China, Hefei 230026, China

S Supporting Information

ABSTRACT: Total chemical synthesis provides a unique approach for the access to uncontaminated, monodisperse, and more importantly, post-translationally modified membrane proteins. In the present study we report a practical procedure for expedient and cost-effective synthesis of small to medium-sized membrane proteins in multimilligram scale through the use of automated Fmoc chemistry. The key finding of our study is that after the attachment of a removable arginine-tagged backbone modification group, the membrane protein segments behave almost the same as ordinary water-soluble peptides in terms of Fmoc solid-phase synthesis, ligation, purification, and mass spectrometry characterization. The efficiency and practicality of the new method is demonstrated by the successful preparation of Ser64-phosphorylated M2 proton channel from influenza A virus and the membrane-embedded domain of an inward rectifier K⁺ channel protein Kir5.1. Functional characterizations of these chemically synthesized membrane proteins indicate that they provide useful and otherwise-difficult-to-access materials for biochemistry and biophysics studies.



INTRODUCTION

Membrane proteins (MPs) comprise 20–30% of the proteomes of most organisms.¹ They perform many essential physiological functions such as signal transduction and molecule transportation.^{2,3} They are also the drug targets of over 50% of modern pharmaceuticals.^{1,4} Therefore MPs have been intensively studied in structural, functional proteomics, and pharmaceutical research.^{5–8} A bottleneck in these studies is that recombinant production of MPs often suffers from low yield, cell toxicity, and incomplete post-translational modifications (PTMs).^{9,10} Chemical protein synthesis¹¹ offers an important alternative route to the production of MPs. This method may be particularly suitable for the studies on small to medium-sized MPs or MP domains.^{12,13} Because chemical synthesis can produce proteins with diverse pre-designed changes with atomic precision,¹⁴ it provides a unique tool for the structural and functional studies of MPs bearing PTMs such as phosphorylation, lipidation or glycosylation.¹⁵ Moreover, chemical synthesis allows precise incorporation of specific labels for advanced biophysical studies.^{16–18}

Despite the promising value of chemical synthesis, only a small number of MPs have been synthesized.^{12,13,15,16,18} A representative example showing the state of the art is the total synthesis of membrane-embedded diacylglycerol kinase DAGK (121 residues).¹³ In the synthesis the segments of MPs are prepared through solid-phase peptide synthesis (SPPS)¹⁹ and

then connected using native chemical ligation.¹¹ Extraordinary difficulty in preparing and handling the transmembrane segments was encountered, because such peptides are very poorly soluble in almost any solvent. Although strategies such as attachment of a solubilizing tag^{20,21} or addition of various organic cosolvents or detergents^{12,13} have been tested, every new preparation of MPs requires tedious and case-specific optimizations.²² Moreover, due to the difficulty of using Fmoc SPPS to prepare either hydrophobic peptides²³ or peptide thioesters,^{24–26} most of the previous MP syntheses relied on the use of Boc SPPS, which unfortunately is not suitable for making MPs carrying acid-sensitive PTMs (e.g., phosphorylation and glycosylation).^{17,27}

Here we present the first Fmoc and potentially general method for total chemical synthesis of small to medium-sized MPs at multimilligram scale (Figure 1a). A critical feature of this method is that we develop a practical removable Arg₄-tagged backbone modification group for MP peptides. Remarkably, with such backbone modification the MP peptides behave as if they are ordinary water-soluble peptides during purification, ligation, as well as for mass spectrum characterizations. This new method, combined with the use of peptide hydrazides in native chemical ligation,^{28,29} allows expedient and

Received: January 10, 2014

Published: February 21, 2014

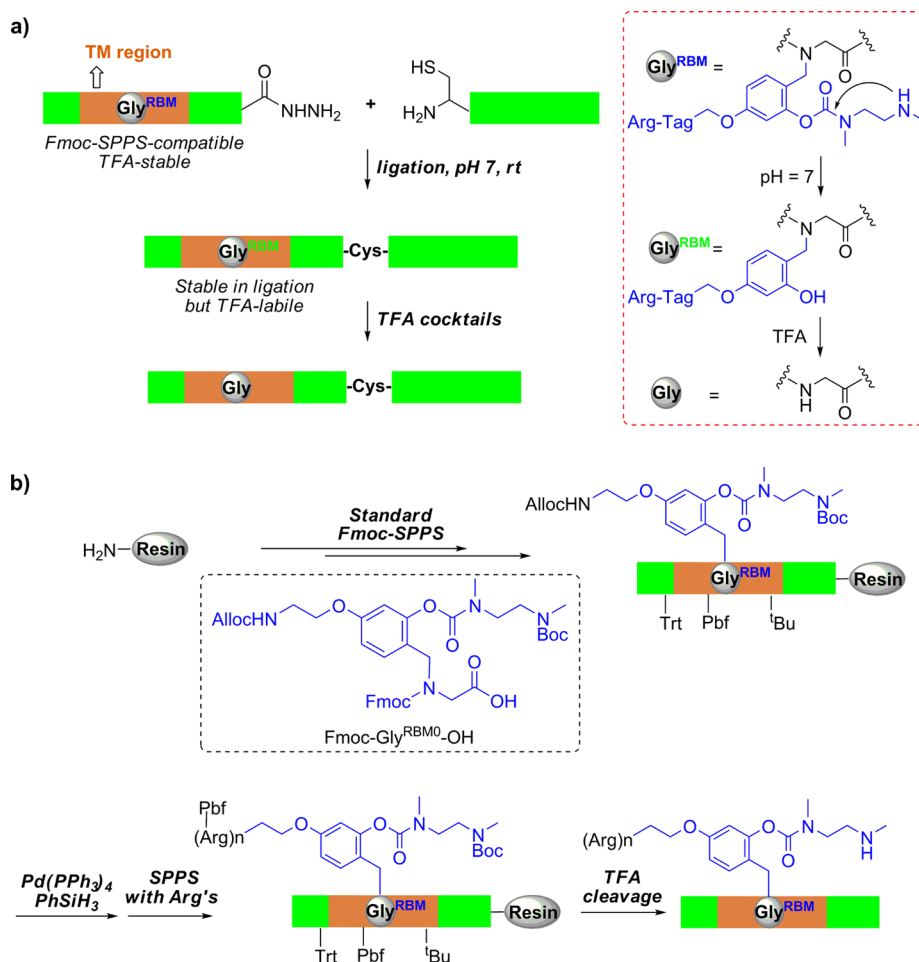


Figure 1. Removable Arg-tagged backbone modification for chemical synthesis of membrane proteins. (a) General concept for the new Fmoc-based method for total chemical synthesis of MPs. (b) The procedure for Fmoc-SPPS synthesis of peptides with removable Arg-tagged backbone modification.

scalable synthesis, purification, and ligation of transmembrane peptides to produce target MPs. Its practicality and usefulness are demonstrated by the successful total synthesis and functional characterizations of Ser64-phosphorylated M2 proton channel from influenza A virus and the membrane-embedded domain of an inward rectifier K⁺ channel protein Kir5.1.

RESULTS AND DISCUSSION

Design of a Backbone Modification Group That Is Removable by TFA. The difficulty revealed by the previous strategies (e.g., C-terminal solubilizing tag²⁰ or addition of organic cosolvents or detergents^{12,13}) led us to hypothesize that a general approach to dissolve MP peptides may require the breaking of their tendency to aggregate via formation of helices or β -sheets. Indeed Kent et al. showed recently that backbone N-methylation of an MP peptide can increase its solubility by disrupting secondary structure formation.³⁰ Unfortunately N-methylation is irreversible, so that the current challenge is to develop a practical approach for removable backbone modification. Considering that a fully assembled MP would be homogeneously soluble only in strong organic acids such as trifluoroacetic acid (TFA),^{23,31} we hypothesized that TFA is the best choice for backbone modification removal in the final step of MP synthesis. This creates a demanding problem because treatment with TFA is already conducted during Fmoc SPPS.

To solve the dilemma we noticed a remarkable property of Johnson's *N*-(2-hydroxy-4-methoxy benzyl) (Hmb) group.³² When attached to peptides, this group can be readily cleaved using TFA. However, if the 2-OH group is acylated, the masked Hmb group is stable toward TFA.³³ We hypothesized that such a subtle change of activity may be used for removable backbone modification (Figure 1a). The Boc-*N*-methyl-*N*-[2-(methylamino)ethyl]-carbamoyl group can be attached to the 2-OH group to prevent the cleavage by TFA during Fmoc SPPS.³⁴ In the process of peptide ligations at neutral pH, the *N*-methyl-*N*-[2-(methylamino)ethyl]carbamoyl group will be autocleaved via intramolecular cyclization.³⁵ Finally, with 2-OH group unprotected, the ligated full-length peptide can be dissolved in TFA to remove the tag and generate the final MP ready for *in vitro* folding.

To test the hypothesis we synthesized the corresponding *N*-tagged Gly residue (Scheme 1 in Supporting Information [SI]). This amino acid can be readily used in automated Fmoc SPPS to synthesize the MP segment (Figure 1b). Note that Gly is one of the six most frequently occurring residues in transmembrane sequences.^{34,36} Thus our strategy of backbone modification at Gly residues should be general for MP synthesis.

We next synthesized a model peptide Ac-AQFRG^{RBM}SLA-NH₂ (1, Figure 2a and Scheme 2 in SI). G^{RBM} denotes the Gly with the removable backbone modification. An Arg₄ tag was

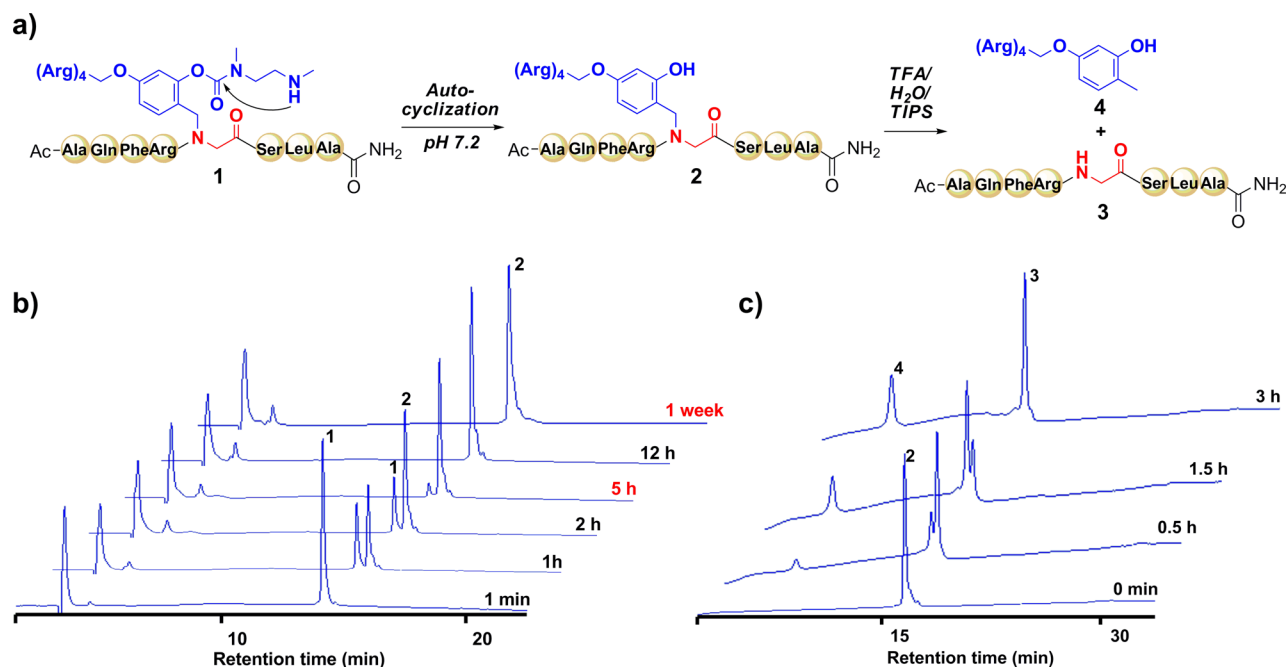


Figure 2. Two-step conversion of a peptide with removable Arg-tagged backbone modification to the native peptide. (a) Conversion of peptide **1** to the native peptide. (b) Analytical RP-HPLC trace for the autocyclization of **1** in the ligation buffer (pH 7.2) at room temperature. (c) Analytical RP-HPLC trace for the removal of the modification group in TFA cocktails at room temperature.

attached to the modification group during Fmoc SPPS (Figure 1b). This peptide was obtained after the treatment with standard TFA cocktail (TFA/TIPS/H₂O). ESI-MS analysis confirmed that 2-OH was capped by the *N*-methyl-*N*-[2-(methyl amino)ethyl]carbamoyl group (Figure 1 in SI).

We dissolved **1** in the neutral aqueous phosphate solution commonly used for native chemical ligation (pH 7.2). A clean conversion of **1** to **2** was observed on analytical RP-HPLC. Peptide **2** possessed a free 2-OH group according to ESI-MS. Over 95% of **1** was converted to **2** after 5 h at room temperature, while the conversion was almost quantitative after 12 h. Moreover, we did not observe any decomposition of **2** after it stayed in the ligation buffer for one week (Figure 2b and Figure 2 in SI). Finally, we dissolved **2** in the TFA/TIPS/H₂O cocktail. RP-HPLC analysis showed that **2** was quantitatively converted to **3** in 3 h.

Performance with Transmembrane Peptides. We chose the fourth transmembrane domain (23-mer) of signal peptide peptidase (SPP, an intramembrane-cleaving protease)³⁰ to examine the solubilizing effect of the removable backbone modification. Seven peptides (SPP4-1 to SPP4-7) were synthesized and labeled by fluorescein isothiocyanate (FITC) to measure the solubility (Figure 3a). The native sequence (SPP4-1) was poorly soluble in 50% aqueous CH₃CN containing 0.1% TFA (Figure 3). Addition of an *N*-terminal Arg₄ tag increased the solubility only by 2-fold (SPP4-2), whereas the removable backbone modification group (without any Arg tag yet) increased the solubility by 5-fold (SPP4-3). When an Arg₂₋₆ tag was added to the backbone modification group, the solubility (SPP4-4, SPP4-5, and SPP4-6) was further increased. Arg₄ provided the best compromise between the solubilizing effect and synthetic cost, leading to an overall increase of solubility by 45-fold (SPP4-5). Finally, when the removable backbone modification group was placed on a different Gly residue (SPP4-7), we observed a similar magnitude of solubilizing effect.

We next measured the solubility of the above peptides in neutral ligation buffer (pH 7.4, 6 M guanidinium-HCl (Gn-HCl), *no detergent*) after they were dissolved overnight. The *N*-methyl-*N*-[2-(methyl amino)ethyl]carbamoyl group was removed under these conditions, and the resulting peptides were denoted as SPP4-1' to SPP4-7'. The solubility of SPP4-1' was measured to be 0.05 mM, which is too low for the ligation reaction (which usually requires 1 mM). *N*-terminal Arg₄-tagged SPP4-2' showed improved solubility (0.37 mM), whereas backbone-modified SPP4-3' was soluble to 0.93 mM. Addition of an Arg_n tag to the backbone modification group again proved critical (SPP4-4' to SPP4-7'). With Arg₄ the solubility of SPP4-5' or SPP4-7' was about 5 mM, corresponding to an increase by ~100 fold over SPP4-1' (Figure 3a).

The above data showed that with the Arg₄-tagged backbone modification, the MP peptides behaved as if they are regular water-soluble protein segments with regard to elution on RP-HPLC, solubility under the ligation conditions, and ionization in mass spectrometry (Figures 5–7 in SI). Backbone modification was necessary for disrupting the secondary structure formation as revealed by the circular dichroism (CD) analysis (Figure 8 in SI). In the CD experiment, SPP4-2 showed a secondary structure similar to that of SPP4-1, whereas SPP4-5 and SPP4-7 exhibited different spectra. Furthermore, during the experiment we observed the aggregation of SPP4-2 when its solution was allowed to stand for 15–30 min. On the other hand, we did not observe any aggregation of SPP4-5 and SPP4-7 after 24 h.

Finally, the ability of the backbone modification group to disrupt secondary structure formation was also advantageous for Fmoc SPPS. As shown in Figure 3c, in the crude SPPS products SPP4-5 was identified as the major component (isolated yield = 15%), whereas SPP4-2 was generated in a much lower yield (isolated yield <5%).

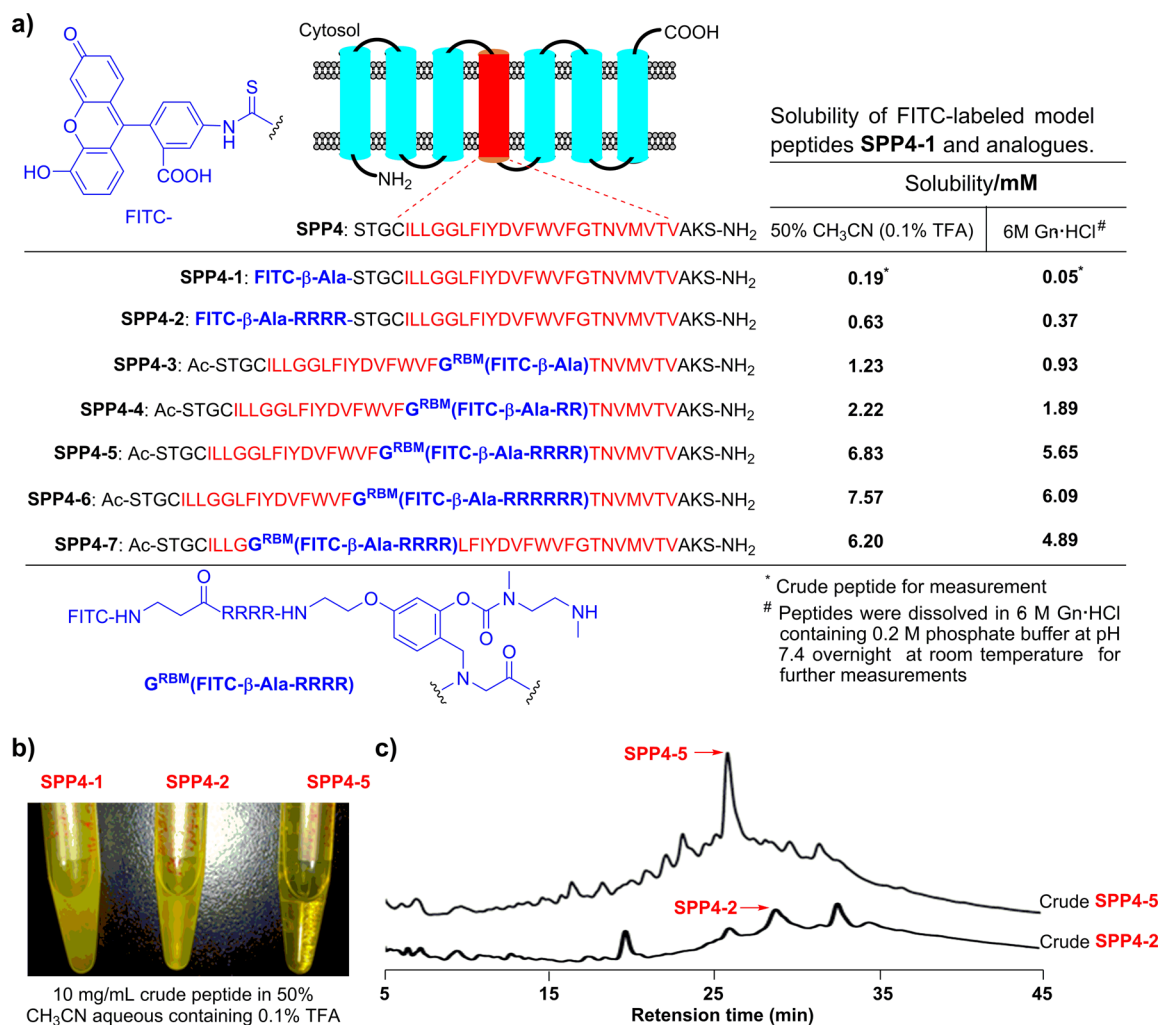


Figure 3. The solubility of FITC-labeled peptides SPP4-1 to SPP4-7. (a) The structures of SPP4 derivatives. (b) The photograph for solubility of crude peptides SPP4-1, SPP4-2 and SPP4-5. (c) RP-HPLC elution profile of crude SPP4-2 and SPP4-5 analogues with a C4 column with a gradient of 30–50% buffer B in buffer A over 40 min.

Total Synthesis of Wild-Type and Ser64-Phosphorylated M2. The M2 proton channel of influenza A virus is a 97-residue homotetrameric integral membrane protein essential for mediating transport of protons across the viral envelope. It has been the subject of numerous structural and functional studies,^{37–39} but some details regarding the role of M2 in virus replication still remain unclear. For instance, M2 carries a number of modifications including palmitoylation, fatty acylation, and phosphorylation,⁴⁰ whose roles in the function, membrane localization, or assembly of M2 remain to be elucidated.⁴¹ In this context chemical synthesis of modified M2 provides useful research reagents.

Kochendoerfer et al. previously used the Boc method to prepare M2.⁴² Here we used the new strategy to synthesize both wild-type and Ser64-phosphorylated M2 through Fmoc chemistry (Figure 4a). The 2-Cl-Trt-NHNH₂ resin was used to prepare M2[1–49, 4Arg-Tag]-NHNH₂ (**5**) by using automated Fmoc SPPS. In this segment Gly34 was modified with the Arg₄-tagged removable modification group. We then used the Nova-PEG Wang resin to prepare M2[50–97] (**6**) also by automated Fmoc SPPS, in which Fmoc-Ser(HPO₃Bzl)-OH was used to install pSer64. Both M2[1–49, 4Arg-Tag]-NHNH₂ and M2[50–97] (bearing either Ser64 (**6**) or pSer64 (**p6**)) were produced as readily soluble peptides (isolated yields = 12%,

20%, 15%) amenable to routine RP-HPLC purification and ESI-MS characterizations (Figure 9 in SI).

The native chemical ligation of M2[1–49, 4Arg-Tag]-NHNH₂ (**5**) and M2[50–97] (**6**) was conducted using the *in situ* NaNO₂ activation/thiolysis protocol.^{28,29} The reaction proceeded smoothly in aqueous Gn·HCl (6 M) *without any organic cosolvent or detergent* to yield the full-length polypeptide in 39% (for Ser64, **7**) or 36% (for pSer64, **p7**) yield (Figure 4a). **7** or **p7** was purified through RP-HPLC and treated with TFA/TIPS/H₂O to remove the backbone modification group in 5 h. The final wild-type (**8**) or Ser64-phosphorylated M2 (**p8**) was obtained through a further RP-HPLC separation in 26% (for Ser64) and 17% (for pSer64) yield. Characterizations of **7** and **8** by ESI-MS and SDS-PAGE are shown in Figure 4b,c. Both wild-type and Ser64-phosphorylated M2's were incorporated into dodecylphosphocholine (DPC) vesicles. The CD spectra of the M2-containing vesicles exhibited evidence of significant α -helical structures with characteristic negative bands at 208 and 222 nm (Figure 4d), suggesting the successful generation of correctly folded M2.

Chemically synthesized full-length M2 proteins were then incorporated into POPC/POPG (POPC: 1-palmitoyl-2-oleoyl-*sn*-glycero-3-phosphocholine; POPG: 1-palmitoyl-2-oleoyl-*sn*-glycero-3-phosphor-(1'-*rac*-glycerol)) bilayers in the presence

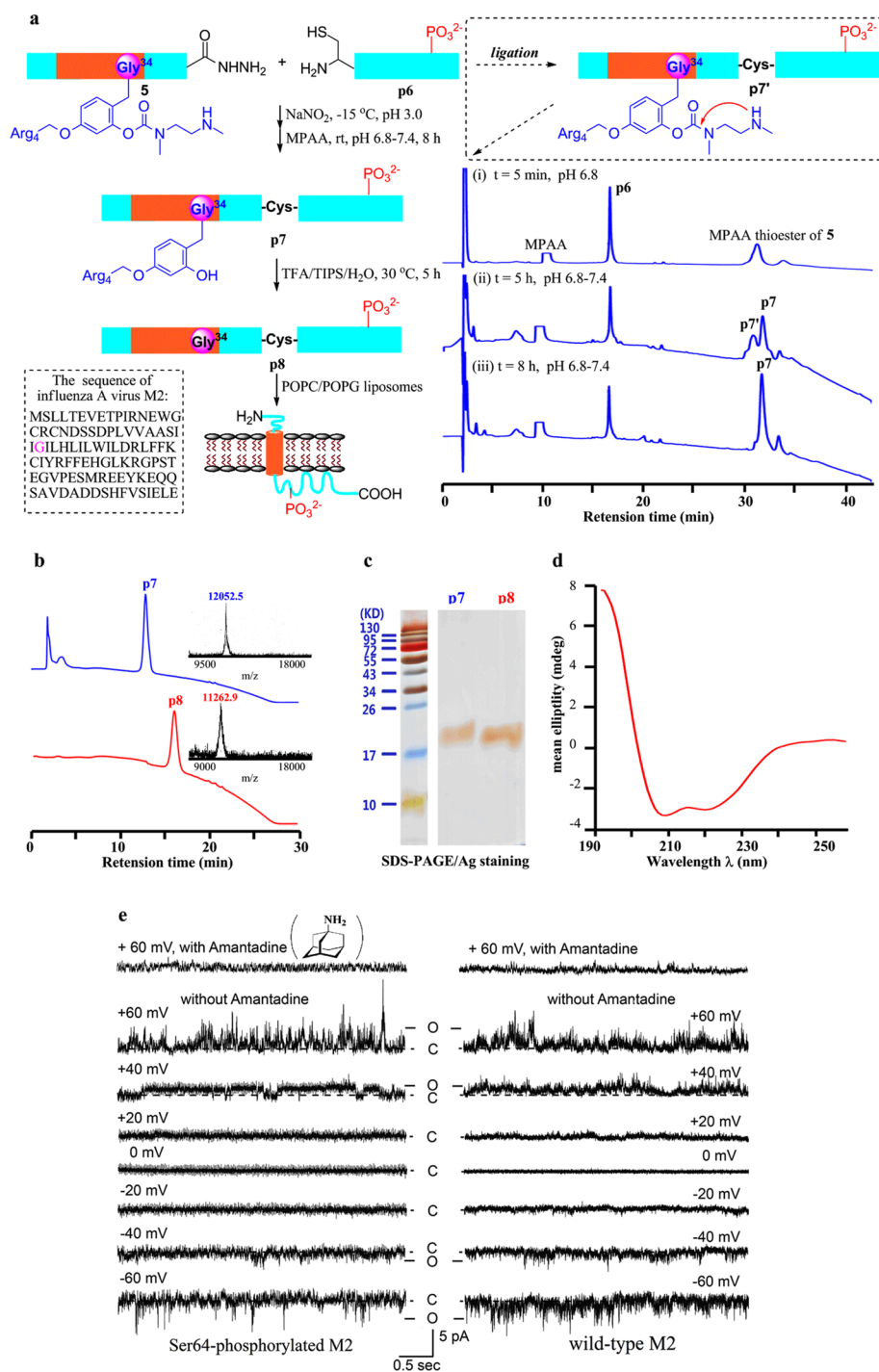


Figure 4. Chemical synthesis and characterizations of wild-type and Ser64-phosphorylated M2. (a) Left: Strategy for chemical synthesis. Right: Analytical data. (b) Analytical data for ligation product Arg-tagged M2-pS64 p7 and the final M2-pS64 p8. Up: RP-HPLC of the purified ligation product Arg-tagged M2-pS64 p7 with a C4 column (4.6 mm × 150 mm) at 56 °C. According to the previous work, the HPLC analysis should be operated at elevated temperatures to facilitate the elution of a membrane peptide from the HPLC column.^{13,30} Inset shows MALDI-TOF-MS of p7. Down: RP-HPLC of the purified native M2-pS64 p8 with a C4 column (4.6 mm × 150 mm) at 56 °C. Inset shows MALDI-TOF-MS of p8. (c) SDS-PAGE/Ag staining analysis: lane left, the ligation product Arg-tagged M2-pS64 p7; lane right, M2-pS64 p8. (d) CD analysis of reconstituted M2-pS64 p8 (5 μM, in a 1 mm quartz cell) in DPC micelles. (e) Single-channel currents of chemical synthetic native and Ser64-phosphorylated M2 protein channels after reconstitution in POPE/POPG (3:1) lipid vesicles. The traces were recorded at various membrane potentials in 5 mM Tris-MOPS, 150 mM NaCl, pH 5.0 both inside and outside. Solid line: opening (O); dotted line: closure (C).

of symmetrical solutions under acidic conditions (5 mM tris(hydroxymethyl)aminomethane (Tris) and 3-morpholinopropanesulfonic acid (MOPS), pH 5.0). Single-channel currents were measured in response to different applied voltages (−60, −40, −20, 0, 20, 40, and 60 mV) (Figure 4e).

Represented traces in Figure 4e show that the channel opens at positive voltages as well as negative ones. Nonetheless, relatively low signal-to-noise ratio was observed in the M2 channel conductance traces, similar to previous reports of reconstituted M2 channels in lipid bilayers, probably due to

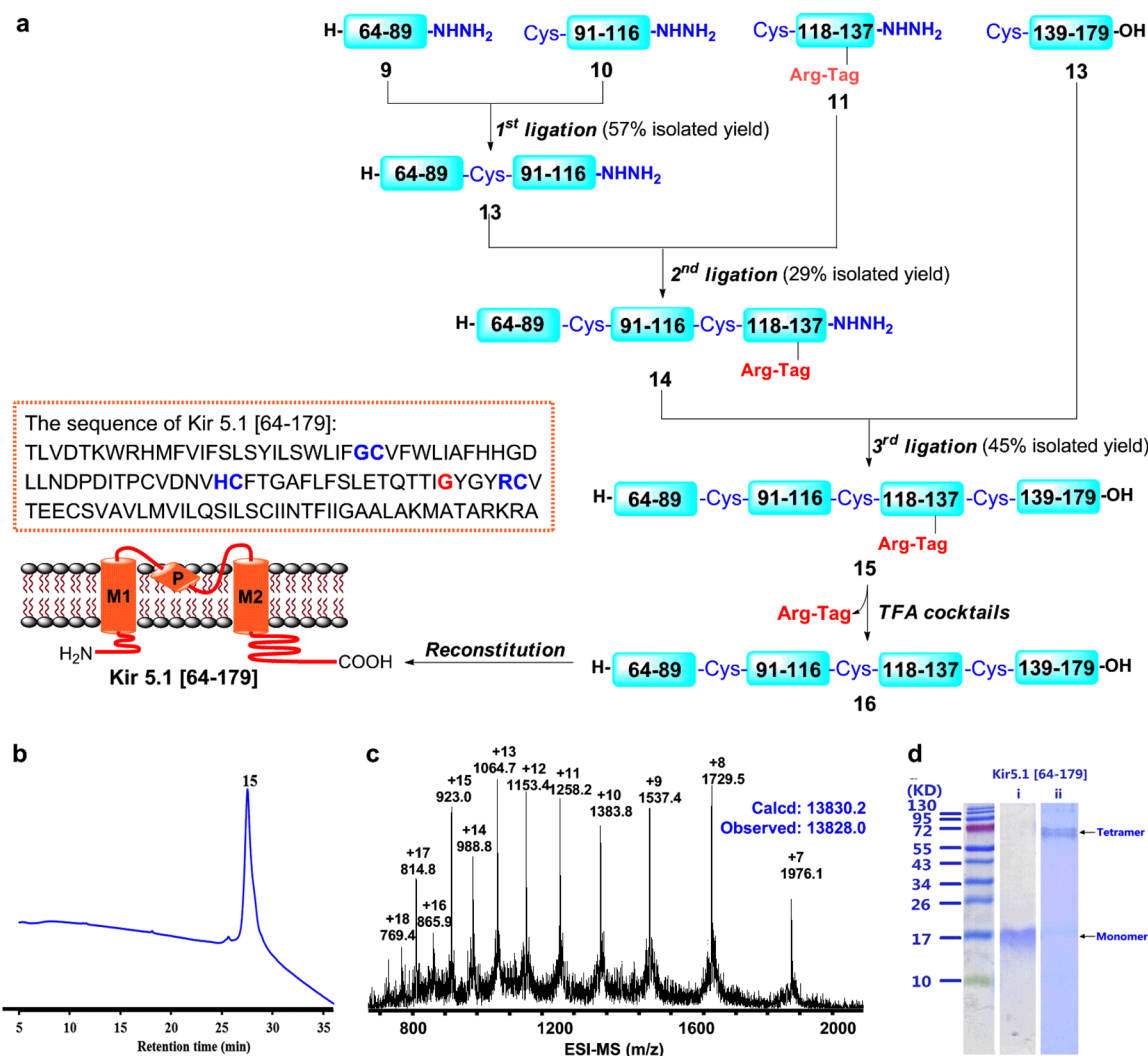


Figure 5. Synthesis of inward rectifier K⁺ channel Kir5.1[64–179]. (a) Kir5.1[64–179] monomer (116 amino acids) is divided into four segments: Kir5.1[64–89]-NHNH₂ 9, Kir5.1[90–116]-NHNH₂ 10, Kir5.1[117–137]-NHNH₂ 11, and Kir5.1[138–179]-OH 12. These four segments were synthesized by Fmoc SPPS and ligated as described in the text. (b) RP-HPLC of the purified product Kir5.1[64–179] 15 with a C4 column (4.6 mm × 150 mm) at 56 °C. Inset shows MALDI-TOF-MS of 15. (c) ESI-MS of 15. The observed baseline shift always occurs (also with blank injections). (d) SDS-PAGE/Ag staining analysis: lane i, the final product Kir5.1[64–179] 16 by TFA cocktails; lane ii, reconstituted tetrameric Kir5.1[64–179] in POPC/POPG liposomes.

disturbance of lipid bilayer integrity under acidic conditions or in nonuniform oligomeric states.⁴³ Then, the channel activity at relatively low potentials (–20, 0, and 20 mV) was not obvious. Meanwhile, control experiments without addition of M2 did not produce any channel activity under the same conditions. To determine the effect of amantadine (an anti-influenza drug through blocking the M2 channel) on chemically synthesized M2, the channel activity was recorded in the absence of amantadine at first. Then aliquots of amantadine solution were added to both chambers to a final concentration of 20 μM. After stirring for about 10 min, the channel activity was measured again. As shown in Figure 4e, the almost total channel blockage in the presence of 20 μM amantadine was observed at a holding potential of +60 mV.

Collectively our results demonstrated that chemically synthesized M2, when incorporated into planar lipid bilayers, can produce single-channel activity after spontaneous fusion at low pH. Comparing the current results of wild-type and Ser64-phosphorylated M2 (Figure 4e), it seemed likely that Ser64-

phosphorylation caused little influence on both the channel activity and the amantadine inhibition effect.

Total Synthesis of Core Transmembrane Domain of Kir5.1. The inward rectifier family of potassium (Kir) channels plays pivotal roles in controlling the excitability of various cells.^{44–46} Kir5.1, a typical Kir channel that is widely expressed in brain and kidney, has been implicated in many physiological and pathological processes such as the modulation of brainstem neurons and the SeSAME/EAST syndrome.⁴⁷ It has been long believed that Kir5.1 formed no functional channel when expressed alone. Yet a functional homomeric Kir5.1 was reported in a rare case, when it was expressed in HEK293T cells with the help of PSD-95, a member of the membrane-associated guanylate kinase (MAGUK) family which can help ion channels to locate on plasma membrane.⁴⁸ This largely overlooked finding raised a hypothesis that the failure to detect functional homomeric Kir5.1 may be due to the lack of ability to locate on the plasma membrane.

To investigate whether pure Kir5.1 can form a functional channel, we synthesized its core transmembrane domain (64–

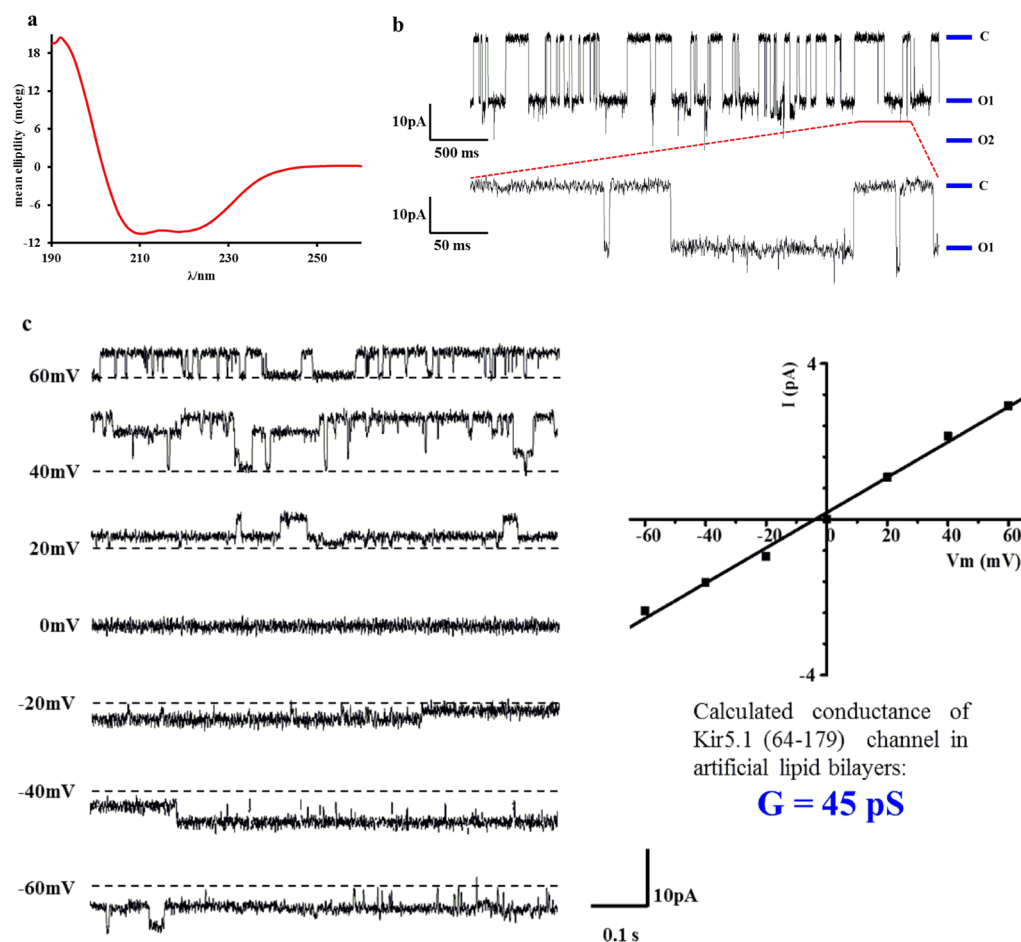


Figure 6. Biophysical characterization of functional Kir5.1[64–179] channels made by total chemical synthesis. (a) CD analysis of functional Kir5.1[64–179] channels ($\sim 10 \mu\text{M}$, in a 1 mm quartz cell). (b) Representative channel activity of the Kir5.1[64–179] channels after reconstitution in POPE/POPG (3:1) lipid vesicles. The traces were recorded at -100 mV in 5 mM HEPES/150 mM KCl (pH 8.0) both inside and outside. A zoom-in of the gating behavior is shown beneath. C: level of channel closure; O1: level 1 of channel opening; O2: level 2 of channel opening. (c) Single-channel conductance of Kir5.1[64–179] in planar lipid bilayers. Left: Single-channel currents were recorded at various membrane potentials. Right: Single-channel conductance was calculated from the current–voltage plot, with the slope conductance of 45 pS. The traces were recorded at -100 mV in 5 mM HEPES/150 mM KCl (pH 8.0) both inside and outside.

179, 116 amino acids) containing two transmembrane helices and a membrane-embedded P-loop. The target protein was divided into four segments, Kir5.1[64–89]-NHNH₂, Kir5.1[90–116]-NHNH₂, Kir5.1[117–137, 4Arg-Tag]-NHNH₂, and Kir5.1[138–179] (Scheme 4 in SI). Three segments (i.e., Kir5.1[64–89]-NHNH₂, Kir5.1[90–116]-NHNH₂, and Kir5.1[138–179]) could be directly prepared in 15%, 20%, and 12% isolated yields. Nonetheless, the P-loop segment Kir5.1[117–137]-NHNH₂ could not be prepared by Fmoc SPPS as the crude peptide was a complex mixture of poorly soluble materials. Only after the Arg4-tagged removable backbone modification group was added at Gly133, could this segment be obtained through automated Fmoc SPPS in 18% isolated yield. The purified peptide was well soluble (Figure 11 in SI).

The four segments were condensed by *N*-to-*C* sequential ligation in aqueous Gn·HCl solutions (isolated yields = 57%, 29%, 45%), producing Kir5.1[64–179] with the Arg₄-tagged backbone modification group in 7.5% overall isolated yield (Figures 12–14 in SI). This molecule was well soluble in aqueous CH₃CN and could be readily isolated by RP-HPLC to >95% purity (Figure 5b,c). The purified, backbone-modified Kir5.1[64–179] powder was then dissolved into TFA/TIS/

H₂O for 5 h at room temperature. The solution was concentrated by N₂ blowing, and the final target protein was obtained through precipitation from cold diethyl ether. The final Kir5.1[64–179] could not be eluted from RP-HPLC. Nonetheless, SDS-PAGE analysis indicated that the final product was the desired protein (Figure 5d).

Synthetic Kir5.1[64–179] was used in the channel reconstitution in unilamellar liposome vesicles with POPC/POPG lipids. Kir5.1[64–179] successfully formed a homogeneous tetramer according to SDS-PAGE (Figure 5d). The CD spectrum of the Kir5.1[64–179]-containing lipids (Figure 6a) showed two minima at 208 and 222 nm, indicating the formation of a well-structured α -helical protein. Channel conductance in the planar lipid bilayer was examined using the proteoliposomes (Kir5.1[64–179] in POPC/POPG), and the single-channel activity was measured at various voltages. Shown in Figure 6b is a 4-s train of recorded current amplitudes with -100 mV voltage applied on the cis side. Uniform current amplitudes of 20 pA or 0 pA were observed with the alternating channel opening or closing. Fast switching between channel opening and closing was also demonstrated in the zoom-in in Figure 6c.

To measure the channel conductance, current amplitudes of Kir5.1[64–179] in the planar lipid bilayer were recorded in duration of 1 s at various voltages (–60, –40, –20, 0, 20, 40, and 60 mV) (Figure 6c). More than one channel was identified in the preparation of Kir5.1[64–179] in the planar lipid bilayer of POPC/POPG. Therefore, the measured current amplitudes exhibited stepwise addition of multiple channels during their openings. Different steps of current amplitudes were estimated from the stepwise sets of data, referring to the predefined baseline. The lowest amplitude level was extracted as the single-channel current amplitude value. For example, two sets of current amplitudes (1.1 and 2.2 pA) were recorded at a voltage of 20 mV, demonstrating a 1.1 pA single-channel current amplitude at 20 mV. The extracted single-channel current amplitudes were plotted against different voltages. The current–voltage was in linear relationship. Slope of the regressed line was 45 pS, representing the single-channel conductance of Kir5.1[64–179] in the planar lipid bilayer of POPC/POPG.

Taken together, the successful channel conductance measurement of synthetic Kir5.1[64–179] indicated that Kir5.1 can form functional homomeric K⁺ channels. This finding supported the previous hypothesis that trafficking and membrane insertion are important limiting steps for channel conductance function, especially using traditionally *in situ* patch-clamp techniques. Our work also indicated that chemical synthesis and reconstitutive refolding provide an effective way to analyze the functions of channel proteins, especially those that cannot be obtained by traditional biological methods or those that exhibit no function *in situ*.

CONCLUSION

The growing research interest in membrane proteins demands a toolbox of approaches for their production. Total chemical synthesis provides a unique technique to the arsenal for the generation of pure, monodisperse, and modified MP samples required for structural and biochemical studies. We showed that, with the removable backbone modification group, the MP peptides behaved almost the same as the peptide segments of water-soluble proteins in terms of Fmoc SPPS, solubility, HPLC elution, and mass characterization. With this method and the technology of using peptide hydrazides as thioester surrogates, small- to middle-sized MPs comprising more than one transmembrane domain can be prepared readily through the use of automated Fmoc chemistry. The efficiency and practicality of the new method was demonstrated by the multimilligram-scale synthesis of the M2 proton channel from influenza A virus and the core transmembrane domain of Kir5.1. These synthetic proteins were free of contamination by other channel-forming proteins derived from cell membranes in recombinant expressions. As a result they provided unique materials for *in vitro* study of MP's biophysical and biochemical properties.

EXPERIMENTAL SECTION

Detailed experimental procedures for the synthesis of compounds, peptides and proteins, their characterization data, and the electrophysiology experiments are given in the Supporting Information.

Synthesis of Gly^{RMB0}-Containing Peptides. The peptide-chain assembly was performed using standard Fmoc-SPPS protocols except for Gly^{RMB0} and the amino acids immediately after Gly^{RMB0}. Gly^{RMB0} residue was coupled using Fmoc-Gly^{RMB0}-OH (2 equiv), HATU (2 equiv), HOAt (2 equiv) and DIEA (4 equiv) for 1.5 h, and then

capped with Ac₂O/DIEA/DMF (1/1/8, v/v/v). After deprotection of Fmoc, the peptide was treated with a double or triple coupling step for the next amino acid and an Ac₂O capping step. After completion of the peptides assembly, Pd(PPh₃)₄/PhSiH₃ in CH₂Cl₂/DMF (1/1, v/v) was added to remove the Alloc group. The deprotection step was repeated once. The Arg-Tag was then coupled by using standard Fmoc-SPPS protocols. The peptide was cleaved from the resin with TFA/PhOH/TIPS/H₂O cocktails.

Chemical Ligation Using Peptide Hydrazides As Thioester Surrogates. Peptide hydrazides were dissolved using 0.2 M phosphate solution containing 6 M Gn·HCl (pH 3.0–3.1) in a Eppendorf reaction tube. The reaction tube was placed in a –15 °C ice–salt bath and the solution was gently agitated by magnetic stirring. 0.5 M NaNO₂ (10–15 equiv) was added, and the solution was gently agitated for 15 min at –15 °C to oxidize the peptide hydrazide to the azide. Subsequently, the phosphate solution containing MPAA (4-mercaptophenylacetic acid, ~100 equiv) and N-terminal Cys-peptide (0.7–1.6 equiv) was added to the reaction mixture to convert the peptide azide to the thioester for native chemical ligation. The tube was removed from the ice–salt bath and warmed to room temperature. The pH of the ligation reaction at the pH to 6.5–7.4 was monitored using a micro pH probe. The ligation was monitored by analytical HPLC and ESI-MS. Note that the autocyclization procedure was performed for 3–5 h under pH 7.4 at ~25–30 °C to completely liberate the phenol group. After completion of ligation, 0.1 M neutral TCEP solution (~100 equiv) was added for 20 min to reduce the ligation system.

Removal of the Backbone Modification by TFA Cocktails. Arg-tagged protein was dissolved in TFA cocktails (TFA/TIPS/H₂O, 95/2.5/2.5, v/v/v). The native protein can be obtained quantitatively for 5 h with TFA. After the cleavage, the reaction mixture was concentrated and precipitated with Et₂O to yield the final product.

Reconstitution in Unilamellar Liposome Vesicles. All lipids used were obtained from Avanti Polar Lipids (Alabaster, AL, USA). Chemically synthesized protein was centrifuged at 14,000 rpm for 10 min to recover the sample that sticks to the tube wall. Into the tube was added 200 μL reconstitution buffer (0.1% SDS, 20 mM Tris, 200 mM NaCl, pH 8.0). The sample was completely dissolved and uniformly dispersed using pipettes. POPC (1.5 mg/mL) and POPG (0.5 mg/mL) were mixed and well dispersed in reconstitution buffer (0.1% SDS, 20 mM Tris, 200 mM NaCl, pH 8.0) through five cycles of liquid nitrogen freezing and thawing at rt. The protein solution was added into the liposome solution to a final molar ratio of 1/600 (protein/lipid). The mixture was rotated at 4 °C for 1 h, and dialyzed for 3 days at 25 °C in Tris buffer (20 mM Tris, 200 mM NaCl, pH 8.0) to completely remove the detergent. To prepare unilamellar liposome vesicles, samples were extruded using a 400 nm polycarbonate membrane by the Avanti Mini-Extruder (Alabaster, AL). Final concentration of protein sample was ~40 μg/mL.

Single-Channel Conductance Measurement in Planar Lipid Bilayer. Channel conductance measurements in planar lipid bilayer were conducted using Ionovation Compact (Osnabrück, Germany). Two polycarbonate compartments in volume of 1.2 mL were separated by a TEFLON foil with 25 μm thickness and 50–100 μm aperture diameter. The premixed liposome (POPC/POPG = 3/1) was employed to paint the aperture. Planar lipid bilayer formation was monitored optically or by capacitance measurements. After successful formation of a stable bilayer in the aperture, proteoliposomes (protein sample in POPC/POPG) were added to the cis chamber next to the bilayer. Fusion of protein and planar lipid bilayer was detected through observation of channel conductance. Working solution (5 mM 4-(2-hydroxyethyl)-1-piperazine-ethanesulfonic acid (HEPES), 150 mM KCl, pH 8.0) was present in both cis- and trans chambers.

Different DC voltage was used to measure channel conductance using an EPC-10 amplifier (HEKA Elektronik). Currents were measured with a 2 kHz low-pass filter at 10 kHz sampling rate. Data was analyzed using the pCLAMP 10.0 software (Axon Instruments). In each measurement at various voltages, current amplitudes were recorded referring to a predefined baseline, based on 50% threshold crossing methods. Current–voltage (*I*–*V*) relationship was plotted

with the measured current amplitudes against different applied voltages. The I - V plot was regressed to a linear line with the slope representing channel conductance of the membrane protein in the planar lipid bilayer.

■ ASSOCIATED CONTENT

● Supporting Information

Experimental details and compound characterizations. This material is available free of charge via the Internet at <http://pubs.acs.org>.

■ AUTHOR INFORMATION

Corresponding Authors

lliu@mail.tsinghua.edu.cn

cltian@ustc.edu.cn

Notes

The authors declare no competing financial interest.

■ ACKNOWLEDGMENTS

This study was supported by the National Basic Research Program of China (973 program, No. 2013CB932800), Chinese Ministry of Science and Technology with the Protein Science Key Projects (2011CB911104), NSFC Grants (91313301, 31100847, and 21225207), the Specialized Research Fund for the Doctoral Program of Higher Education (Grant No. 20120002130004), and China Postdoctoral Science Foundation (Nos. 2012M520009, 2013T60098).

■ REFERENCES

- (1) Bill, R. M.; Henderson, P. J.; Iwata, S.; Kunji, E. R.; Michel, H.; Neutze, R.; Newstead, S.; Poolman, B.; Tate, C. G.; Vogel, H. *Nat. Biotechnol.* **2011**, *29*, 335–340.
- (2) Gouaux, E.; Mackinnon, R. *Science* **2005**, *310*, 1461–1465.
- (3) Venkatakrishnan, A. J.; Deupi, X.; Lebon, G.; Tate, C. G.; Schertler, G. F.; Babu, M. M. *Nature* **2013**, *494*, 185–194.
- (4) Yildirim, M. A.; Goh, K. I.; Cusick, M. E.; Barabási, A. L.; Vidal, M. *Nat. Biotechnol.* **2007**, *25*, 1119–1126.
- (5) White, S. H. *Nature* **2009**, *459*, 344–346.
- (6) Rosenbaum, D. M.; Rasmussen, S. G.; Kobilka, B. K. *Nature* **2009**, *459*, 356–363.
- (7) Lappano, R.; Maggiolini, M. *Nat. Rev. Drug Discovery* **2011**, *10*, 47–60.
- (8) Neuzi, P.; Giselbrecht, S.; Länge, K.; Huang, T. J.; Manz, A. *Nat. Rev. Drug Discovery* **2012**, *11*, 620–632.
- (9) Schwarz, D.; Junge, F.; Durst, F.; Frölich, N.; Schneider, B.; Reckel, S.; Sobhanifar, S.; Dötsch, V.; Bernhard, F. *Nat. Protoc.* **2007**, *2*, 2945–2957.
- (10) Junge, F.; Schneider, B.; Reckel, S.; Schwarz, D.; Dötsch, V.; Bernhard, F. *Cell. Mol. Life Sci.* **2008**, *65*, 1729–1755.
- (11) (a) Dawson, P. E.; Muir, T. W.; Clark-Lewis, I.; Kent, S. B. H. *Science* **1994**, *266*, 776–779. (b) Nilsson, B. L.; Soellner, M. B.; Raines, R. T. *Annu. Rev. Biophys. Biomol. Struct.* **2005**, *34*, 91–118. (c) Haase, C.; Seitz, O. *Angew. Chem., Int. Ed.* **2008**, *47*, 1553–1556.
- (12) (a) Bianchi, E.; Ingenito, R.; Simon, R. J.; Pessi, A. *J. Am. Chem. Soc.* **1999**, *121*, 7698–7699. (b) Clayton, D.; Shapovalov, G.; Maurer, J. A.; Dougherty, D. A.; Lester, H. A.; Kochendoerfer, G. G. *Proc. Natl. Acad. Sci. U.S.A.* **2004**, *101*, 4764–4769.
- (13) Lahiri, S.; Brehs, M.; Olschewski, D.; Becker, C. F. *Angew. Chem., Int. Ed.* **2011**, *50*, 3988–3992.
- (14) (a) Kent, S. B. H. *Chem. Soc. Rev.* **2009**, *38*, 338–351. (b) Devaraneni, P. K.; Komarov, A. G.; Costantino, C. A.; Devereaux, J. J.; Matulef, K.; Valiyaveetil, F. I. *Proc. Natl. Acad. Sci. U.S.A.* **2013**, *110*, 15698–15703. (c) Matulef, K.; Komarov, A. G.; Costantino, C. A.; Valiyaveetil, F. I. *Proc. Natl. Acad. Sci. U.S.A.* **2013**, *110*, 17886–17891.
- (15) (a) Tolbert, T. J.; Wong, C. H. *J. Am. Chem. Soc.* **2000**, *122*, 5421. (b) Huse, M.; Holford, M. N.; Kuriyan, J.; Muir, T. W. *J. Am. Chem. Soc.* **2000**, *122*, 8337. (c) Asahina, Y.; Kamitori, S.; Takao, T.; Nishi, N.; Hojo, H. *Angew. Chem., Int. Ed.* **2013**, *52*, 9733–9737.
- (16) Kochendoerfer, G. G.; Jones, D. H.; Lee, S.; Oblatt-Montal, M.; Opella, S. J.; Montal, M. *J. Am. Chem. Soc.* **2004**, *126*, 2439–2446.
- (17) Muralidharan, V.; Muir, T. W. *Nat. Methods* **2006**, *3*, 429–438.
- (18) Valiyaveetil, F. I.; Leonetti, M.; Muir, T. W.; Mackinnon, R. *Science* **2006**, *314*, 1004–1007.
- (19) Kent, S. B. H. *Annu. Rev. Biochem.* **1988**, *57*, 957–989.
- (20) (a) Sato, T.; Saito, Y.; Aimoto, S. *J. Pept. Sci.* **2005**, *11*, 410–416. (b) Johnson, E. C.; Kent, S. B. H. *Tetrahedron Lett.* **2007**, *48*, 1795–1799. (c) Johnson, E. C.; Malito, E.; Shen, Y.; Rich, D.; Tang, W. J.; Kent, S. B. H. *J. Am. Chem. Soc.* **2007**, *129*, 11480–11490.
- (21) (a) Tan, Z.; Shang, S.; Danishefsky, S. J. *Proc. Natl. Acad. Sci. U.S.A.* **2011**, *108*, 4297–4302. (b) Huang, Y. C.; Li, Y. M.; Chen, Y.; Pan, M.; Li, Y. T.; Yu, L.; Guo, Q. X.; Liu, L. *Angew. Chem., Int. Ed.* **2013**, *52*, 4858–4862.
- (22) Olschewski, D.; Becker, C. F. *Mol. Biosyst.* **2008**, *4*, 733–740.
- (23) Coin, I.; Beyermann, M.; Bienert, M. *Nat. Protoc.* **2007**, *2*, 3247–3256.
- (24) Pattabiraman, V. R.; Bode, J. W. *Nature* **2011**, *480*, 471–479.
- (25) Zheng, J. S.; Chang, H. N.; Wang, F. L.; Liu, L. *J. Am. Chem. Soc.* **2011**, *133*, 11080–11083.
- (26) Zheng, J. S.; Tang, S.; Huang, Y. C.; Liu, L. *Acc. Chem. Res.* **2013**, *46*, 2475–2484.
- (27) Shin, Y.; Winans, K. A.; Backes, B. J.; Kent, S. B. H.; Ellman, J. A.; Bertozzi, C. R. *J. Am. Chem. Soc.* **1999**, *121*, 11684–11689.
- (28) Fang, G. M.; Li, Y. M.; Shen, F.; Huang, Y. C.; Li, J. B.; Lin, Y.; Cui, H. K.; Liu, L. *Angew. Chem., Int. Ed.* **2011**, *50*, 7645–7649.
- (29) Zheng, J. S.; Tang, S.; Qi, Y. K.; Wang, Z. P.; Liu, L. *Nat. Protoc.* **2013**, *8*, 2483–2495.
- (30) Johnson, E. C.; Kent, S. B. H. *J. Am. Chem. Soc.* **2006**, *128*, 7140–7141.
- (31) Speers, A. E.; Wu, C. C. *Chem. Rev.* **2007**, *107*, 3687–3714.
- (32) Johnson, T.; Quibell, M.; Owen, D.; Sheppard, R. C. *J. Chem. Soc., Chem. Commun.* **1993**, 369–372.
- (33) Quibell, M.; Turnell, W. G.; Johnson, T. *J. Org. Chem.* **1994**, *59*, 1745–1750.
- (34) (a) Wahlstrom, K.; Planstedt, O.; Undén, A. *Tetrahedron Lett.* **2008**, *49*, 3779–3781. (b) Wahlstrom, K.; Planstedt, O.; Undén, A. *Tetrahedron Lett.* **2008**, *49*, 3921–3924.
- (35) Saari, W. S.; Schwering, J. E.; Lyle, P. A.; Smith, S. J.; Engelhardt, E. L. *J. Med. Chem.* **1990**, *33*, 97–101.
- (36) Eilers, M.; Shekar, S. C.; Shieh, T.; Smith, S. O.; Fleming, P. J. *Proc. Natl. Acad. Sci. U.S.A.* **2000**, *97*, 5796–5801.
- (37) Schnell, J. R.; Chou, J. J. *Nature* **2008**, *451*, 591–596.
- (38) Stouffer, A. L.; Acharya, R.; Salom, D.; Levine, A. S.; Di Costanzo, L.; Soto, C. S.; Tereshko, V.; Nanda, V.; Stayrook, S.; DeGrado, W. F. *Nature* **2008**, *451*, 596–599.
- (39) Rossman, J. S.; Jing, X.; Leser, G. P.; Lamb, R. A. *Cell* **2010**, *142*, 902–913.
- (40) Holsinger, L. J.; Shaughnessy, M. A.; Micko, A.; Pinto, L. H.; Lamb, R. A. *J. Virol.* **1995**, *69*, 1219–1225.
- (41) Grantham, M. L.; Wu, W. H.; Lalime, E. N.; Lorenzo, M. E.; Klein, S. L.; Pekosz, A. *J. Virol.* **2009**, *83*, 8655–8661.
- (42) Kochendoerfer, G. G.; Salom, D.; Lear, J. D.; Wilk-Orescan, R.; Kent, S. B. H.; DeGrado, W. F. *Biochemistry* **1999**, *38*, 11905–11913.
- (43) (a) Duff, K. C.; Ashley, R. H. *Virology* **1992**, *190*, 485–489. (b) Tosteson, M. T.; Pinto, L. H.; Holsinger, L. J.; Lamb, R. A. *J. Membr. Biol.* **1994**, *142*, 117–126.
- (44) Hibino, H.; Inanobe, A.; Furutani, K.; Murakami, S.; Findlay, I.; Kurachi, Y. *Physiol. Rev.* **2010**, *90*, 291–366.
- (45) Bavro, V. N.; De Zorzi, R.; Schmidt, M. R.; Muniz, J. R.; Zubcevic, L.; Sansom, M. S.; Vénien-Bryan, C.; Tucker, S. J. *Nat. Struct. Mol. Biol.* **2012**, *19*, 158–163.
- (46) Tao, X.; Avalos, J. L.; Chen, J.; MacKinnon, R. *Science* **2009**, *326*, 1668–1674.

- (47) Paulais, M.; Bloch-Faure, M.; Picard, N.; Jacques, T.; Ramakrishnan, S. K.; Keck, M.; Sohet, F.; Eladari, D.; Houillier, P.; Lourdel, S.; Teulon, J.; Tucker, S. J. *Proc. Natl. Acad. Sci. U.S.A.* **2011**, *108*, 10361–10366.
- (48) Tanemoto, M.; Fujita, A.; Higashi, K.; Kurachi, Y. *Neuron* **2002**, *34*, 387–97.